JACS
JOURNAL OF THE AMERICAN CHEMICAL SOCIETY

Article

pubs.acs.org/JACS

An Electrochemical Study of Frustrated Lewis Pairs: A Metal-Free Route to Hydrogen Oxidation

Elliot J. Lawrence,[†] Vasily S. Oganesyan,[†] David L. Hughes,[†] Andrew E. Ashley,*[,‡] and Gregory G. Wildgoose*[,†]

[†]School of Chemistry, University of East Anglia, Norwich Research Park, Norwich, NR4 7TJ, United Kingdom
[‡]Department of Chemistry, Imperial College London, South Kensington, London, SW7 2AZ, United Kingdom

Supporting Information

ABSTRACT: Frustrated Lewis pairs have found many applications in the heterolytic activation of H_2 and subsequent hydrogenation of small molecules through delivery of the resulting proton and hydride equivalents. Herein, we describe how H_2 can be preactivated using classical frustrated Lewis pair chemistry and combined with in situ nonaqueous electrochemical oxidation of the resulting borohydride. Our approach allows hydrogen to be cleanly converted into two protons and two electrons in situ, and reduces the potential (the required energetic driving force) for nonaqueous H_2 oxidation by 610 mV (117.7 kJ mol^{-1}). This significant energy reduction opens routes to the development of nonaqueous hydrogen energy technology.

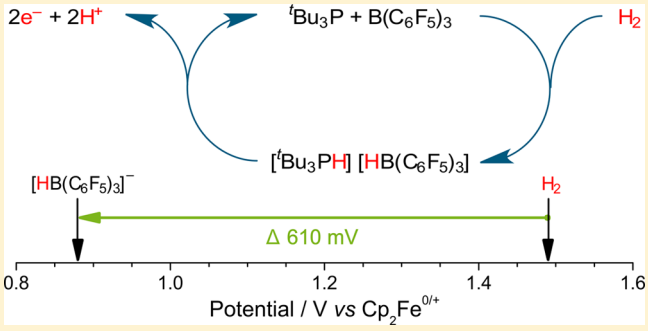

INTRODUCTION

H_2 is attractive as a "clean" fuel source, leading to a vast body of literature concerned with fuel cell technology.[1,2] In the absence of an appropriate electrocatalyst (defined as a system that reduces the overpotential, the required energetic driving force, and/or increases the rate of electron transfer), the nonaqueous oxidation of H_2 to liberate two protons and two electrons is slow, requiring large overpotentials (often in excess of 1000 mV vs $Cp_2Fe^{0/+}$ at carbon electrodes) and producing broad, ill-defined oxidation waves. Conventional, predominantly aqueous, fuel cells surmount this problem by using precious metals such as Pt as a catalytic electrode material.[3−5] Because Pt electrodes are often used for both half-reactions of the fuel cell (H_2 oxidation and O_2 reduction), the high costs of these metals and limited availability present significant problems for large-scale use. Of course, this is true for a multitude of catalyzed processes, and, as a result, huge efforts have been made to find inexpensive and abundant alternatives to precious metals.[6]

The majority of molecular electrocatalysts for H_2 oxidation or production have taken inspiration from the hydrogenase enzymes that are found in nature.[7−9] The active site of hydrogenase enzymes features a coordinatively unsaturated [FeFe] or [NiFe] metal center with pendant Lewis base groups in close proximity. These enzymes are able to overcome the high energy cost that is required to heterolytically cleave H_2 (318.0 kJ mol^{-1} in MeCN)[10,11] by virtue of the strong hydricity of the metal center and the strong proton acceptor ability of the pendant base. Several groups, notably DuBois and co-workers, have reported bioinspired molecular electrocatalysts for H_2 oxidation using nickel[12−14] and iron[15−17] metals that mimic the role of hydrogenases. Rauchfuss and co-workers took an alternative approach to H_2 oxidation electrocatalysis, using unsaturated iridium complexes with redox-active noninnocent amidophenolate ligands.[18,19] They were able to induce Lewis acidity on the metal center through a ligand-centered oxidation, allowing the formation of a H_2 adduct that is susceptible to deprotonation by a weakly coordinating base. All of these approaches still use metal-containing catalysts, and there are a greater number of literature reports that focus on biomimetic electrocatalysts for the reverse process, H_2 production via proton reduction, than for H_2 oxidation.[9] The greatest challenges in developing H_2 energy technologies still remain, to find systems that are catalytic in terms of hydrogen bond cleavage, that operate at low overpotentials (i.e., that are "electrocatalytic"), that are metal-free and/or employ inexpensive, readily available electrode materials such as carbon, and that are facile and economic to synthesize.

In this Article, we build on our recent studies of the electrochemistry of electron-deficient Lewis acid boranes,[20−22] and introduce a new approach that combines classical frustrated Lewis pair (FLP) chemistry to "pre-activate" H_2 with nonaqueous electrochemical oxidation of the resulting borohydride. To the best of our knowledge, this is the first time that FLPs have been directly used for the electrochemical activation of small molecules. Aqueous-phase borohydride ($[BH_4]^-$) electrooxidation has been reviewed extensively because of its potential for fuel cell applications;[3−5] however, in this respect,

Received: January 16, 2014
Published: April 2, 2014

   dx.doi.org/10.1021/ja500477g | J. Am. Chem. Soc. 2014, 136, 6031−6036

the field has so far been devoid of nonaqueous applications. Since the pioneering work of Stephan's group in 2006,[23] research involving FLP chemistry has grown rapidly. The "unquenched" reactivity, arising from a suitable combination of a sterically bulky Lewis acid and a Lewis base, has been shown to heterolytically cleave H_2 resulting in a hydride adduct of the Lewis acid and a protonated Lewis base.[6,23−28] Boranes are typically, but not exclusively, employed as the Lewis acid component.[26,27,29−35] Following the heterolytic cleavage of H_2, using an FLP system, the majority of literature reports focus on delivering the resulting hydride via heterolytic B−H bond cleavage to activate/reduce other small molecules such as imines, enamines, nitriles,[36,37] and even CO_2.[38,39] The only prior report that indirectly combines electrochemistry with FLP systems, that we are aware of, is by Stephan and co-workers, who used mono- and bis-ferrocenylphosphines in an FLP system, to observe the quasi-reversible oxidation of the ferrocene redox "label" and the reduction of the proton on the phosphonium moiety.[40]

We begin by exploring the electrochemical properties of Stephan's paradigm ^{t}Bu$_3$P/B(C$_6$F$_5$)$_3$ FLP system[29] and seek to use this approach to demonstrate the conversion of H_2 into two protons and two electrons (Figure 1a). After elucidating the

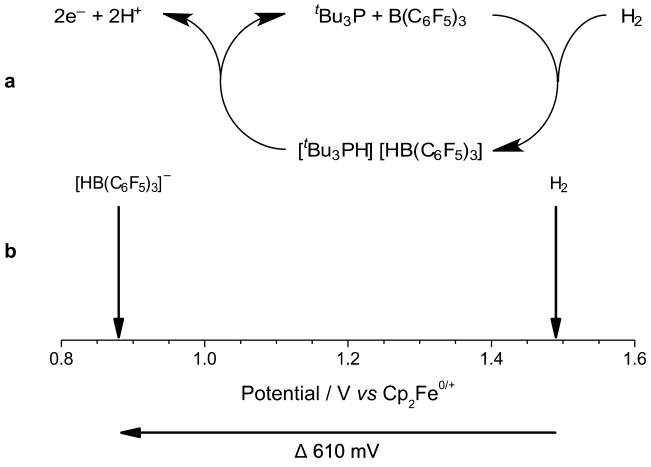

Figure 1. Proposed electrooxidation of the H_2-activated ^{t}Bu$_3$P/B(C$_6$F$_5$)$_3$ frustrated Lewis pair (FLP) results in (a) the generation of two protons and two electrons, and (b) an effective diminution in the potential required for H_2 oxidation by 610 mV (117.7 kJ mol^{-1}) in CH_2Cl_2.

kinetic and mechanistic electrochemical behavior of this classical FLP system, we report that our approach reduces the oxidation potential of H_2 in nonaqueous solvents by 610 mV (117.7 kJ mol^{-1}) on carbon electrodes, a significant and large reduction in the required energetic driving force (Figure 1b). This new route to H_2 oxidation is metal-free, operating on inexpensive, ubiquitous, carbon electrodes. While this initial finding proffers a significant enabling step toward economically viable energy technologies, we can also identify some areas for improvement in this pioneering study of a classical FLP system. Fortunately, FLPs are versatile and inherently tunable systems, with evermore-improved H_2-activating FLPs reported apace. It is envisaged that the introduction of our innovative electrochemical frustrated Lewis pair approach, herein, will open new avenues to researchers for further development in small molecule activation and clean energy technologies.

RESULTS AND DISCUSSION

Initial Electrochemical Studies. An authentic sample of [^{n}Bu$_4$N][HB(C$_6$F$_5$)$_3$] ([^{n}Bu$_4$N]**1**), containing the hydridic component (**1**$^-$) of the FLP H_2-cleavage step, was prepared and its structure established by X-ray crystallography and spectroscopic methods (see Supporting Information sections S1.2, S2, and S3). The authentic borohydride sample allowed a detailed electrochemical study into the redox behavior of **1**$^-$ to be undertaken. The direct voltammetric oxidation of [^{n}Bu$_4$N]**1**, at varying concentrations, was performed at a macrodisk glassy carbon electrode (GCE) using cyclic voltammetry (Figures 2 and 3).

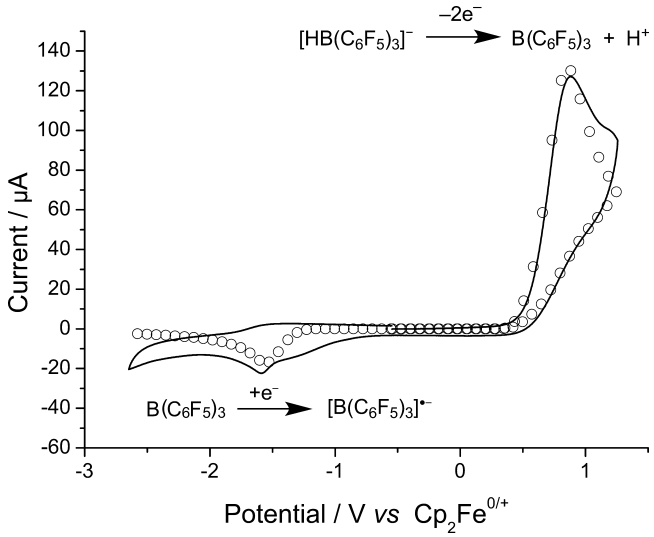

Figure 2. Cyclic voltammograms of a 4.9 mM solution of [^{n}Bu$_4$N]**1** in CH_2Cl_2 recorded at voltage scan rates of 1000 mV s^{-1} over the full scan range on a glassy carbon electrode (GCE). Solid lines are experimental data; "O" are best fit simulated data. The oxidation wave corresponds to the oxidation of **1**$^-$, while the reduction wave corresponds to reduction of regenerated B(C$_6$F$_5$)$_3$.[21,22]

A weakly coordinating electrolyte system comprising 0.05 M [^{n}Bu$_4$N][B(C$_6$F$_5$)$_4$] in CH_2Cl_2 was selected for all electrochemical studies to minimize the decomposition of B(C$_6$F$_5$)$_3$.[20,41] On sweeping the potential anodically at a scan

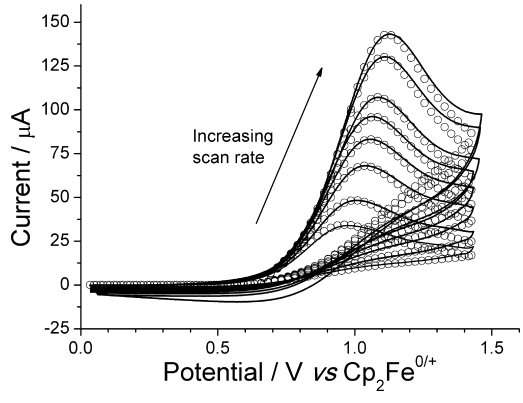

Figure 3. Cyclic voltammograms of a 4.9 mM solution of [^{n}Bu$_4$N]**1** in CH_2Cl_2 recorded at voltage scan rates of 50, 100, 200, 300, 400, 500, 750, and 1000 mV s^{-1} on a glassy carbon electrode (GCE). Solid lines are experimental data; "O" are best fit simulated data (see text).

dx.doi.org/10.1021/ja500477g | J. Am. Chem. Soc. 2014, 136, 6031−6036

rate of 100 mV s^{-1}, an oxidative wave was initially observed with a peak potential of (E_p) +0.88 ± 0.01 V vs $Cp_2Fe^{0/+}$, and no corresponding (quasi-reversible) reduction peak was observed upon reversing the scan direction. However, a small irreversible reduction wave was observed at −1.59 V vs $Cp_2Fe^{0/+}$ (Figure 2) that we assign to the reduction of some catalytically regenerated parent Lewis acid, $B(C_6F_5)_3$, from our previous studies.[21,22] The small size of this reduction wave is likely as a result of subsequent protonolysis of the parent $B(C_6F_5)_3$ (see below). The observed voltammetry can be explained by the mechanism proposed in Figure 4, which is

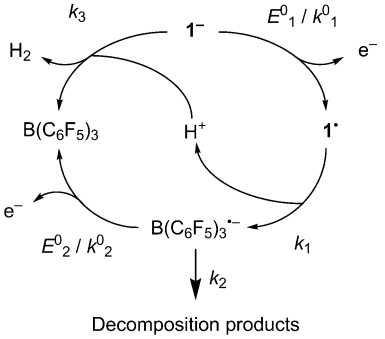

Figure 4. Proposed mechanism and associated thermodynamic and kinetic parameters used in simulation of the voltammetric oxidation of $\mathbf{1}^-$ at a GCE (standard reduction potential, E^0/V; standard electron transfer rate constant, k^0/cm s^{-1}; chemical rate constant, k/s^{-1}).

supported by a good fit between simulation and experiment (Figures 2 and 3) and detailed chemical and density functional theory (DFT) studies described below. The globally optimized parameters describing the oxidation of $\mathbf{1}^-$ were obtained from digital simulation of the CVs and are given in Table 1, while the parameters describing the reduction of $B(C_6F_5)_3$ are taken from our previous work.[21]

Stoichiometric Reactions. When $[^nBu_4N]\mathbf{1}$ is subjected to chemical oxidation using a stoichiometric amount of the single-electron oxidant $[NO][PF_6]$ in CH_2Cl_2, effervescence is observed. Analysis of the reaction mixture headspace using gas chromatography with a thermal conductivity detector (GC-TCD) revealed that H_2 gas was evolved.

Two mechanisms for H_2 production are possible: (i) the reaction of electrogenerated H^+ with the parent $\mathbf{1}^-$, as we propose (Figure 4), or (ii) by a reaction between transient $[(C_6F_5)_3BH]^\bullet$ ($\mathbf{1}^\bullet$) intermediates acting as $H^\bullet$ donors. To exclude the possibility of the latter pathway, we conducted a control experiment using an authentic $H^\bullet$-donor, $^nBu_3SnH$, which was mixed with 4-bromobenzophenone in equimolar quantities in a sealed NMR tube and allowed to react under UV light. ^1H NMR characterization of the products revealed the formation of benzophenone via the radical dehalogenation of 4-bromobenzophenone by $H^\bullet$. However, when $[^nBu_4N]\mathbf{1}$ is stoichiometrically oxidized in the presence of $[NO][PF_6]$ and an equimolar amount of 4-bromobenzophenone, the latter is recovered in quantitative yield by NMR; no benzophenone is detected in the reaction mixture. Furthermore, effervescence is observed when **1** and a stoichiometric amount of Jutzi's strong oxonium acid, $[H(OEt_2)_2][B(C_6F_5)_4]$,[42] are combined in CH_2Cl_2. H_2 gas is once again detected in the reaction headspace, supporting the proposed proton-mediated H_2 evolution mechanism. Note that in either case ^{11}B NMR characterization of the product mixture reveals a number of peaks in the range −0.5 to −7.0 ppm consistent with our previous characterization of the complex products of B-$(C_6F_5)_3$ decomposition (such as $[(C_6F_5)_3BCl]^-$, $[(C_6F_5)_2BCl_2]^-$, $[(C_6F_5)_2BHCl]^-$, and $[(C_6F_5)_3BH]^-$ and F^- abstraction products from the $[PF_6]^-$ anion in the former case; see ref 21 for details).[21]

Conclusively, when a sample of deuterated $[^nBu_4N][DB(C_6F_5)_3]$ ($[^nBu_4N]\mathbf{1}^D$) is subjected to bulk electrolytic oxidation at a glassy carbon electrode in the presence of $^tBu_3P$, an intense triplet resonance is seen in the $^{31}P\{^1H\}$ NMR spectrum at 59.6 ppm (J = 65.8 Hz), which corresponds to $[^tBu_3P-D]^+$. Because the only possible source of D^+ is from the oxidation of $\mathbf{1}^{D-}$, this strongly supports the proposed mechanism in Figure 4, wherein B−D/B−H bond cleavage in $\mathbf{1}^{D\bullet}$ results in the formation of a deuteron/proton, respectively. Further support for the proposed mechanism is obtained from DFT computational calculations (Supporting Information section S5). The calculated bond energies for parent $\mathbf{1}^-$ and $\mathbf{1}^\bullet$ reveal that bond scission is significantly enhanced upon electrooxidation.

In Situ Electrochemical Studies during the Heterolytic Cleavage of H_2 by a Frustrated Lewis Pair. With a detailed understanding of the redox chemistry of $\mathbf{1}^-$, we proceeded toward in situ electrochemical studies of the archetypal $^tBu_3P/B(C_6F_5)_3$ system during the FLP cleavage of H_2. The kinetics of heterolytic H_2 cleavage by this FLP system are much slower than the rate of electrooxidation when monitored using ^{11}B, ^{19}F, and ^{31}P NMR spectroscopy (see Supporting Information Figures S8−10). The heterolytic cleavage of H_2 by the FLP was complete after 12 h, but even within 1 h evidence of H_2 cleavage by the FLP could be observed in the NMR spectra.

Table 1. Globally Optimized Best-Fit Thermodynamic and Kinetic Parameters Obtained from Digital Simulation of Voltammetric Data for $[^nBu_4N]\mathbf{1}$ at a GCE, Following the Mechanism Proposed in Figure 4

	redox parameters		
redox process	E^0/V vs $Cp_2Fe^{0/+}$	$k^0/10^{-3}$ cm s^{-1}	charge transfer coefficient
$\mathbf{1}^- \rightleftharpoons \mathbf{1}^\bullet + e^-$	+1.13 ± 0.05	13 ± 2	0.74 ± 0.1
$B(C_6F_5)_3^{\bullet-} \rightleftharpoons B(C_6F_5)_3 + e^-$	−1.79 ± 0.01[a]	1.3 ± 0.3[a]	0.50 ± 0.05[a]
chemical step		rate constant	
$\mathbf{1}^\bullet \rightarrow B(C_6F_5)_3^{\bullet-} + H^+$		$k_1 > 1 \times 10^{13}$ s^{-1}	
$B(C_6F_5)_3^{\bullet-} \rightarrow$ decomposition products		$k_2 > 6.1$ s^{-1}[a]	
$\mathbf{1}^- + H^+ \rightarrow B(C_6F_5)_3 + H_2$		$k_3 = (1.50 \pm 0.25) \times 10^7$ M^{-1} s^{-1}	

[a]Parameters taken from our previous studies of $B(C_6F_5)_3$.[21]

dx.doi.org/10.1021/ja500477g | J. Am. Chem. Soc. 2014, 136, 6031−6036

Figure 5 shows the resulting voltammetry recorded after a 1:1 solution of $^{t}Bu_3P$:$B(C_6F_5)_3$ (containing ferrocene as an internal reference) was sparged with H_2 gas for 1 h.

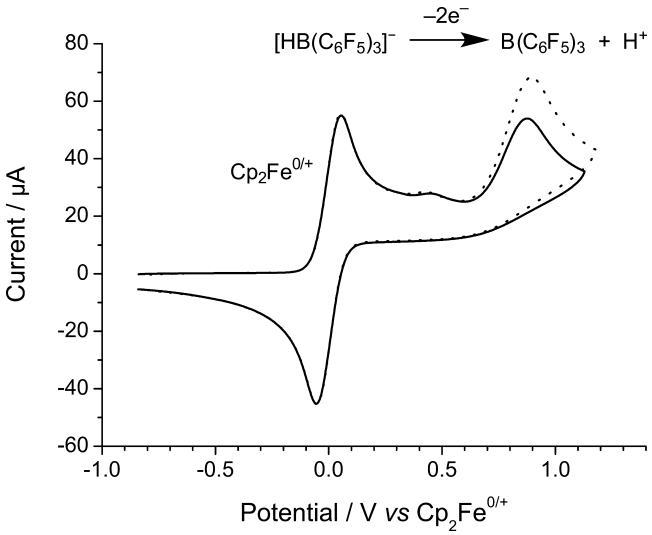

Figure 5. Cyclic voltammogram of a 5 mM solution of $^{t}Bu_3P$ and $B(C_6F_5)_3$ in CH_2Cl_2 solution, at a GCE, after being exposed to a 1 h sparge with H_2 (black line). Addition of authentic $[^{n}Bu_4N]\mathbf{1}$ (dotted line) to the sample confirms that the observed oxidation wave corresponds to the H_2-activated product. The cyclic voltammograms were taken in the presence of a Cp_2Fe internal reference at a voltage scan rate of 100 mV s^{-1}.

Reassuringly, we observe the characteristic oxidation wave of $\mathbf{1}^-$, which is identical to that of $[^{n}Bu_4N]\mathbf{1}$. Confirmation of this was shown by a proportional increase in the oxidation current at +0.88 V vs $Cp_2Fe^{0/+}$ when the solution was spiked with an authentic sample of $[^{n}Bu_4N]\mathbf{1}$ (Figure 5). H_2 is itself oxidized sluggishly, with a broad, ill-defined wave at ca. +1.49 V vs $Cp_2Fe^{0/+}$ in CH_2Cl_2 on a glassy carbon electrode (see Supporting Information Figure S13). Hence, by employing combined electrochemical FLP approach, the oxidation of H_2 now occurs with a ca. 610 mV (117.7 kJ mol^{-1}) diminution in the required driving force. Note that $[^{t}Bu_3PH]^+$ is not redox active at the potentials studied. However, some oxidation of unreacted $^{t}Bu_3P$ is apparent as a small oxidation wave at +0.44 V vs $Cp_2Fe^{0/+}$.

To investigate whether this electrochemical FLP system can be recycled, that is, is catalytic in the Lewis acid, the following experiments were performed: A CH_2Cl_2 solution containing a 5 mM 1:1 mixture of $B(C_6F_5)_3$:$^{t}Bu_3P$ and 0.1 M $[^{n}Bu_4N][B(C_6F_5)_4]$ electrolyte was sealed under an atmosphere of H_2 for 12 h at room temperature to ensure that the FLP heterolytic cleavage of H_2 was complete. This solution was then subjected to bulk electrolysis using a glassy carbon felt electrode until all of the $\mathbf{1}^-$ had been oxidized. The solution was again sealed under H_2 with the addition of another equimolar amount of $^{t}Bu_3P$, for a further 12 h, and the electrolysis was repeated. Disappointingly, upon a second and third electrolytic cycle, no evidence for the regeneration of the parent borane, $B(C_6F_5)$, and subsequent reformation of $\mathbf{1}^-$ could be observed, consistent with the ^{11}B NMR characterization of the products of chemical oxidation of $\mathbf{1}^-$ and the fact that we only observe a small reductive peak corresponding to $B(C_6F_5)_3$ upon cyclic voltammetric oxidation of $[^{n}Bu_4N]\mathbf{1}$, described above. Clearly, the $B(C_6F_5)_3^{\bullet-}$ intermediate produced upon oxidation undergoes significant side reactions with the solvent, and any $B(C_6F_5)_3$ generated is susceptible to protonolysis by the H^+, which is liberated alongside the formation of $B(C_6F_5)_3^{\bullet-}$. Note that "buffering" the electrolyte using excess phosphine Lewis base to prevent unwanted protonolysis reactions is not possible in this system as the Lewis base is itself redox active at potentials similar to that of $\mathbf{1}^-$.

Given that this is the first study of the electrochemistry of FLPs toward H_2 activation, and choosing the archetypal $B(C_6F_5)_3/^{t}Bu_3P$ seems a logical starting point for these investigations, it is perhaps not surprising that this system is not optimal. However, these findings are important as they demonstrate that the electrochemical FLP approach has genuine promise for metal-free H_2 oxidation at significantly lower oxidative potentials, with obvious synthetic and energy applications. This study also allows us to immediately identify areas for future improvement in electrochemical FLP systems: (i) Competing protonation of $\mathbf{1}^-$ regenerates H_2 and reduces the overall efficiency of the process (although the H_2 may be subsequently recycled in future systems), but protonolysis also leads to unwanted decomposition of the Lewis acidic borane. Lewis acids that are resistant to protonolysis are required. (ii) The $B(C_6F_5)_3^{\bullet-}$ radical anion intermediate generated during oxidation of the parent borohydride is susceptible to reaction with the solvent, again preventing the system from being recycled. Steric and/or electronic protection of any radical anion intermediates is required. (iii) The kinetics of H_2 splitting by the FLP are rate determining versus rapid electron transfer in this classical FLP system. Fortunately, improved combinations of novel Lewis acids and bases continue to develop rapidly in conventional FLP chemistry. The inherent "tuneability" of FLP properties thus offers enormous potential for the further development of electrochemical FLP systems, and promising candidates that may overcome all of these obstacles are currently under investigation.

■ CONCLUSIONS

We have characterized the complex nonaqueous redox chemistry of $\mathbf{1}^-$ for the first time. By combining FLP preactivation of H_2 with electrochemical oxidation of the resultant Lewis acid hydride, we have reduced the potential that is required for nonaqueous H_2 oxidation by 610 mV (117.7 kJ mol^{-1}) at readily available carbon electrodes. This is a significant energy reduction without the use of metals (precious or otherwise), which opens hitherto unexplored routes to the development of economically viable H_2-based energy technologies and H_2-activation chemistries. We have also demonstrated that our electrochemical FLP approach is possible with in situ H_2 activation using a classical FLP system. Our work has identified specific areas for future development to further extend the scope and possibilities of this electrochemical FLP chemistry. Patent protection for the intellectual property described herein has been sought.

■ EXPERIMENTAL DETAILS

General Considerations. Commercially available reagents were purchased from Sigma-Aldrich (Gillingham, UK) and used without further purification unless stated otherwise. All synthetic reactions and manipulations were performed under a rigorously dry N_2 atmosphere (BOC Gases) using standard Schlenk-line techniques on a dual manifold vacuum/inert gas line or either a Saffron or an MBraun glovebox. All glassware was flame-dried under vacuum before use.

dx.doi.org/10.1021/ja500477g | J. Am. Chem. Soc. 2014, 136, 6031−6036

Anhydrous solvents were dried via distillation over appropriate drying agents. All solvents were sparged with nitrogen gas to remove any trace of dissolved oxygen and stored in ampules over activated 4 Å molecular sieves. $^{n}Bu_4NCl$ and $NOPF_6$ were purchased from Alfa Aesar. $^{n}Bu_4NCl$ was recrystallized from acetone prior to use. H_2 gas (99.995%) was purchased from BOC gases and passed through drying columns containing P_4O_{10} and 4 Å molecular sieves. D_2 gas was generated in situ from the reaction of Na with degassed D_2O (99.9%, Cambridge Isotope Laboratories Inc.); it was passed through a drying column containing P_4O_{10}. Deuterated NMR solvents ([D_6]DMSO, 99.9%; CDCl3, 99.8%; C_6D_6, 99.5%) were purchased from Cambridge Isotope Laboratories Inc. and were dried over P_4O_{10}, degassed using a triple freeze−pump−thaw cycle, and stored over activated 4 Å molecular sieves. $B(C_6F_5)_3$,[43] $[^{n}Bu_4N][B(C_6F_5)_4]$,[44,45] $[H(OEt_2)_2][B(C_6F_5)_4]$,[42] and $^{t}Bu_3P$[46] were prepared according to literature methods. [TMP−D][D−$B(C_6F_5)_3$] was prepared using an adapted literature method,[47] which is detailed in the Supporting Information. Synthesis and characterization of compounds $[^{n}Bu_4N]$**1** and $[^{n}Bu_4N]$**1**^{D} are detailed in the Supporting Information.

NMR spectra were recorded using either a Bruker Avance DPX-300 MHz or a Bruker Avance DPX-500 MHz spectrometer. Chemical shifts are reported in ppm and are referenced relative to appropriate standards: ^{19}F ($CFCl_3$); ^{11}B ($Et_2O{\cdot}BF_3$); ^{31}P (85% H_3PO_4). IR spectra were recorded using a PerkinElmer μ-ATR Spectrum II spectrometer. Sample headspace analysis was performed using a PerkinElmer Clarus 580 gas chromatograph coupled with a thermal conductivity detector (GC-TCD). Retention time for H_2 gas was calibrated using a standard sample. Electrochemical measurements were performed in CH_2Cl_2 containing 0.05−0.10 M $[^{n}Bu_4N][B(C_6F_5)_4]$ as a weakly coordinating electrolyte salt using either a PGSTAT 302N or a PGSTAT 30 computer-controlled potentiostat (Autolab, Utrecht, The Netherlands) in an inert atmosphere three-electrode cell that was designed in-house (see the Supporting Information for further details). Digital simulation of voltammetric data was performed using the commercially available DigiElch Pro software package (v.7). Diffraction intensities of $[^{n}Bu_4N]$**1** were recorded using a AFC12 Kappa 3 CCD diffractometer (at the EPSRC UK National Crystallography Service) equipped with Mo Kα radiation and confocal mirrors monochromator (for further details, see the Supporting Information).

■ ASSOCIATED CONTENT

Ⓢ Supporting Information

Synthetic details, NMR characterization, X-ray crystallography, electrochemistry, and DFT calculations. This material is available free of charge via the Internet at http://pubs.acs.org.

■ AUTHOR INFORMATION

Corresponding Authors

a.ashley@imperial.ac.uk

g.wildgoose@uea.ac.uk

Notes

The authors declare no competing financial interest.

■ ACKNOWLEDGMENTS

The research leading to these results has received funding from the European Research Council under the ERC Grant Agreement no. 307061 (ERC-St-G-PiHOMER). We thank the EPSRC UK National Crystallography Service at the University of Southampton for the collection of the crystallographic data for $[^{n}Bu_4N]$**1**.[48] G.G.W. and A.E.A. thank the Royal Society for financial support via University Research Fellowships. E.J.L. thanks the EPSRC for financial support via a DTA studentship under the grant code EP/J500409.

■ REFERENCES

(1) Dunn, S. *Int. J. Hydrogen Energy* **2002**, *27*, 235−264.

(2) Turner, J.; Sverdrup, G.; Mann, M. K.; Maness, P.-C.; Kroposki, B.; Ghirardi, M.; Evans, R. J.; Blake, D. *Int. J. Energy Res.* **2008**, *32*, 379−407.

(3) Santos, D. M. F.; Sequeira, C. A. C. *Renewable Sustainable Energy Rev.* **2011**, *15*, 3980−4001.

(4) Merino-Jiménez, I.; Ponce de León, C.; Shah, A. A.; Walsh, F. C. *J. Power Sources* **2012**, *219*, 339−357.

(5) Ma, J.; Choudhury, N. A.; Sahai, Y. *Renewable Sustainable Energy Rev.* **2010**, *14*, 183−199.

(6) *Catalysis Without Precious Metals*; Bullock, R. M., Ed.; Wiley: New York, 2010.

(7) Vignais, P. M.; Billoud, B. *Chem. Rev.* **2007**, *107*, 4206−4272.

(8) Tard, C.; Pickett, C. J. *Chem. Rev.* **2009**, *109*, 2245−2274.

(9) DuBois, D. L.; Bullock, R. M. *Eur. J. Inorg. Chem.* **2011**, *2011*, 1017−1027.

(10) Curtis, C. J.; Miedaner, A.; Ellis, W. W.; DuBois, D. L. *J. Am. Chem. Soc.* **2002**, *124*, 1918−1925.

(11) Wayner, D. D.; Parker, V. D. *Acc. Chem. Res.* **1993**, *26*, 287−294.

(12) Yang, J. Y.; Bullock, R. M.; Shaw, W. J.; Twamley, B.; Fraze, K.; Rakowski DuBois, M.; DuBois, D. L. *J. Am. Chem. Soc.* **2009**, *131*, 5935−5945.

(13) Goff, A. L.; Artero, V.; Jousselme, B.; Tran, P. D.; Guillet, N.; Métayé, R.; Fihri, A.; Palacin, S.; Fontecave, M. *Science* **2009**, *326*, 1384−1387.

(14) Yang, J. Y.; Chen, S.; Dougherty, W. G.; Kassel, W. S.; Bullock, R. M.; DuBois, D. L.; Raugei, S.; Rousseau, R.; Dupuis, M.; Rakowski DuBois, M. *Chem. Commun.* **2010**, *46*, 8618−8620.

(15) Camara, J. M.; Rauchfuss, T. B. *J. Am. Chem. Soc.* **2011**, *133*, 8098−8101.

(16) Camara, J. M.; Rauchfuss, T. B. *Nat. Chem.* **2012**, *4*, 26−30.

(17) Liu, T.; DuBois, D. L.; Bullock, R. M. *Nat. Chem.* **2013**, *5*, 228−233.

(18) Ringenberg, M. R.; Kokatam, S. L.; Heiden, Z. M.; Rauchfuss, T. B. *J. Am. Chem. Soc.* **2008**, *130*, 788−789.

(19) Ringenberg, M. R.; Nilges, M. J.; Rauchfuss, T. B.; Wilson, S. R. *Organometallics* **2010**, *29*, 1956−1965.

(20) Ashley, A. E.; Herrington, T. J.; Wildgoose, G. G.; Zaher, H.; Thompson, A. L.; Rees, N. H.; Kraemer, T.; O'Hare, D. *J. Am. Chem. Soc.* **2011**, *133*, 14727−14740.

(21) Lawrence, E. J.; Oganesyan, V. S.; Wildgoose, G. G.; Ashley, A. E. *Dalton Trans.* **2013**, *42*, 782−789.

(22) Cummings, S. A.; Iimura, M.; Harlan, C. J.; Kwaan, R. J.; Trieu, I. V.; Norton, J. R.; Bridgewater, B. M.; Jaekle, F.; Sundararaman, A.; Tilset, M. *Organometallics* **2006**, *25*, 1565−1568.

(23) Welch, G. C.; Juan, R. R. S.; Masuda, J. D.; Stephan, D. W. *Science* **2006**, *314*, 1124−1126.

(24) Stephan, D. W. *Org. Biomol. Chem.* **2012**, *10*, 5740−5746.

(25) Stephan, D. W. *Org. Biomol. Chem.* **2008**, *6*, 1535.

(26) Stephan, D. W. *Dalton Trans.* **2009**, 3129.

(27) Stephan, D. W.; Erker, G. *Angew. Chem., Int. Ed.* **2010**, *49*, 46−76.

(28) Erker, G. *Dalton Trans.* **2011**, *40*, 7475−7483.

(29) Welch, G. C.; Stephan, D. W. *J. Am. Chem. Soc.* **2007**, *129*, 1880−1881.

(30) Jiang, C.; Blacque, O.; Fox, T.; Berke, H. *Dalton Trans.* **2011**, *40*, 1091.

(31) Lu, Z.; Cheng, Z.; Chen, Z.; Weng, L.; Li, Z. H.; Wang, H. *Angew. Chem., Int. Ed.* **2011**, *50*, 12227−12231.

(32) Herrington, T. J.; Thom, A. J. W.; White, A. J. P.; Ashley, A. E. *Dalton Trans.* **2012**, *41*, 9019.

(33) Voss, T.; Mahdi, T.; Otten, E.; Fröhlich, R.; Kehr, G.; Stephan, D. W.; Erker, G. *Organometallics* **2012**, *31*, 2367−2378.

(34) Binding, S. C.; Zaher, H.; Chadwick, F. M.; O'Hare, D. *Dalton Trans.* **2012**, *41*, 9061−9066.

(35) Travis, A. L.; Binding, S. C.; Zaher, H.; Arnold, T. A. Q.; Buffet, J.-C.; O'Hare, D. *Dalton Trans.* **2013**, *42*, 2431.

(36) Chase, P. A.; Jurca, T.; Stephan, D. W. *Chem. Commun.* **2008**, 1701.

(37) Stephan, D. W.; Greenberg, S.; Graham, T. W.; Chase, P.; Hastie, J. J.; Geier, S. J.; Farrell, J. M.; Brown, C. C.; Heiden, Z. M.; Welch, G. C.; Ullrich, M. *Inorg. Chem.* **2011**, *50*, 12338−12348.
(38) Tran, S. D.; Tronic, T. A.; Kaminsky, W.; Michael Heinekey, D.; Mayer, J. M. *Inorg. Chim. Acta* **2011**, *369*, 126−132.
(39) Ashley, A. E.; Thompson, A. L.; O'Hare, D. *Angew. Chem., Int. Ed.* **2009**, *48*, 9839−9843.
(40) Ramos, A.; Lough, A. J.; Stephan, D. W. *Chem. Commun.* **2009**, 1118−1120.
(41) Geiger, W. E.; Barrière, F. *Acc. Chem. Res.* **2010**, *43*, 1030−1039.
(42) Jutzi, P.; Müller, C.; Stammler, A.; Stammler, H.-G. *Organometallics* **2000**, *19*, 1442−1444.
(43) Lancaster, S. J. *ChemSpider Synthetic Pages* **2003**, DOI: 10.1039/SP215.
(44) Martin, E.; Hughes, D. L.; Lancaster, S. J. *Inorg. Chim. Acta* **2010**, *363*, 275−278.
(45) LeSuer, R. J.; Buttolph, C.; Geiger, W. E. *Anal. Chem.* **2004**, *76*, 6395−6401.
(46) Srivastava, R. C. *J. Chem. Res., Synop.* **1985**, 330−331.
(47) Sumerin, V.; Schulz, F.; Nieger, M.; Leskelä, M.; Repo, T.; Rieger, B. *Angew. Chem., Int. Ed.* **2008**, *47*, 6001−6003.
(48) Gale, P. A.; Coles, S. *Chem. Sci.* **2012**, 683.